Parameterized gait pattern generator based on linear inverted pendulum model with natural ZMP references

YA-FANG HO, TZUU-HSENG S. LI, PING-HUAN KUO and YAN-TING YE

Department of Electrical Engineering, aiRobots Laboratory, National Cheng Kung University, Tainan 70101, Taiwan;
e-mail: makinosakuya@hotmail.com, thsli@mail.ncku.edu.tw, coll22000@hotmail.com, s1020jason@gmail.com

Abstract

This paper presents a parameterized gait generator based on linear inverted pendulum model (LIPM) theory, which allows users to generate a natural gait pattern with desired step sizes. Five types of zero moment point (ZMP) components are proposed for formulating a natural ZMP reference, where ZMP moves continuously during single support phases instead of staying at a fixed point in the sagittal and lateral plane. The corresponding center of mass (CoM) trajectories for these components are derived by LIPM theory. To generate a parameterized gait pattern with user-defined parameters, a gait planning algorithm is proposed, which determines related coefficients and boundary conditions of the CoM trajectory for each step. The proposed parameterized gait generator also provides a concept for users to generate gait patterns with self-defined ZMP references by using different components. Finally, the feasibility of the proposed method is validated by the experimental results with a teen-sized humanoid robot, David, which won first place in the sprint event at the 20th Federation of International Robot-soccer Association (FIRA) RoboWorld Cup.

1 Introduction

Nowadays, humanoid robot has become one of most popular topics in robotics research. However, it is still a challenging task for biped robots to walk stably, and many algorithms such as neural fuzzy network (Kim *et al.*, 2005; Ferreira *et al.*, 2011), policy gradient reinforcement learning (Tedrake *et al.*, 2004; Li *et al.*, 2011; Su *et al.*, 2011), Q-learning algorithm (Park *et al.*, 2004; Hu *et al.*, 2008), and central pattern generator (CPG) (Endo *et al.*, 2008; Nassour *et al.*, 2013; Farzaneh *et al.*, 2014; Li *et al.*, 2015) have been utilized to generate a stable biped gait pattern. CPG is a bio-inspired neural network that generates rhythmic signals to imitate a nervous system. Its center system can be used to coordinate each actuator so as to produce a walking motion with rhythmic signals. However, there is no intuitive relationship between the periodic signals and the motions. Thus, it is difficult to generate a parameterized gait pattern with desired step sizes using CPG.

Instead of using machine learning algorithms to generate a gait pattern, some research has utilized the linear inverted pendulum model (LIPM) (Kajita *et al.*, 2001; Taskiran *et al.*, 2010; Shin & Kim, 2014) with a zero moment point (ZMP) reference to generate a stable walking reference. In LIPM theory, the robot model is simplified into an inverted pendulum model with its center of mass (CoM) constrained at a constant height. Due to the linear property, the robot model can be easily implemented on real robots at low computational cost. Erbatur and Kurt (2009) proposed a natural reference generation method using LIPM and a natural ZMP reference. However, the CoM trajectory proposed by Erbatur was approximated using the Fourier series instead of an analytical solution for the relationship between CoM and ZMP, and

the step sizes for each step are identical. Hence, this trajectory is unsuitable for parameterized gait pattern generation. In contrast, the analytical solutions of the CoM trajectory are derived for parameterized gait pattern generation in this paper.

According to the concept proposed by Erbatur and Kurt (2009), a ZMP reference with ZMP moving forward slightly within single support phases (SSP) is regarded as a natural ZMP reference. To formulate a natural ZMP reference, we further propose five types of ZMP components in this paper. Analytical solutions for these ZMP components are derived to obtain a corresponding CoM trajectory of the natural ZMP reference. Moreover, a gait planning algorithm is presented to determine the boundary conditions for each step so that a parameterized gait pattern can be generated with user-defined parameters. With the proposed method, users can design a parameterized gait pattern with desired step sizes for each step. The period of a step and the period of double support phase (DSP) is also adjustable. Thus, average velocity of the gait pattern is also user-controllable.

This paper is organized as follows. The basic concepts of LIPM are introduced in Section 2. Then, five types of ZMP components are presented and their corresponding CoM trajectories are derived, where the natural ZMP reference composed of proposed ZMP components is introduced. In Section 3, the parameterized gait planning algorithm is presented. Section 4 illustrates the simulation and experimental results. Finally, conclusions and future work are described in Section 5.

2 Natural ZMP and center of mass trajectories based on the linear inverted pendulum model method

In this section, the relationship between the ZMP and CoM of the LIPM theory is introduced first. Then, different types of ZMP references are derived to acquire corresponding CoM trajectories based on the relationship.

2.1 Basic concept of linear inverted pendulum model

In LIPM theory (Erbatur & Kurt, 2009), the robot model is simplified as a point mass supported by a massless leg like an inverted pendulum. Since the leg is assumed to be massless for simplification, mass of the leg should be much less than the mass of robot's upper body. If this assumption is not achieved, the modeling error may affect the stability. The mass of the robot is assumed to concentrate at a point, which is the CoM of the robot. Moreover, the height of CoM z_c is assumed to be constant, so the CoM is constrained on a fixed-height plane while walking. The last assumption yields a linear system in which the motion of CoM can be decoupled in the sagittal plane and lateral plane. Thus, considering that the control torque at the contact point is assigned 0, the equations of motion of the CoM in the sagittal plane and the lateral plane are expressed as follows:

$$\begin{bmatrix} \ddot{x} \\ \ddot{y} \end{bmatrix} = \frac{g}{z_c} \begin{bmatrix} x \\ y \end{bmatrix} \tag{1}$$

where g is the gravity constant, and x and y the coordinates of the CoM in the sagittal and lateral planes, respectively.

To guarantee walking stability, ZMP, which is a widely used criterion for stable biped walking (Vukobratović & Stepanenko, 1972; Choi *et al.*, 2004; Kajita *et al.*, 2006, 2007), is considered. In order to achieve zero moment at the contact point as shown in Figure 1, torque caused by gravity should be balanced by torque caused by acceleration of the CoM. Thus, a torque balance equation in both sagittal and lateral planes is obtained as follows:

$$\begin{bmatrix} \ddot{x} \\ \ddot{y} \end{bmatrix} = \frac{g}{z_c} \begin{bmatrix} x \\ y \end{bmatrix} - \frac{g}{z_c} \begin{bmatrix} p \\ q \end{bmatrix} = \omega_n^2 \begin{bmatrix} x \\ y \end{bmatrix} - \omega_n^2 \begin{bmatrix} p \\ q \end{bmatrix} \tag{2}$$

where ω_n is defined as $\sqrt{g/z_c}$, and p and q the coordinates of ZMP in the sagittal and lateral planes, respectively.

It is noted that (2) also presents the relationship between ZMP and CoM, and the CoM trajectory can be derived by assigning a suitable ZMP trajectory to (2). For simplicity, the following only presents the derivation of the CoM trajectory in the sagittal plane, namely $x(t)$, and the CoM trajectory in the lateral
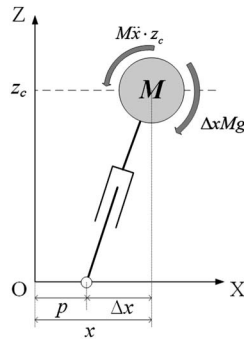
Figure 1   Torque balance for linear inverted pendulum model in the sagittal plane

plane $y(t)$ can be obtained in the same way. Applying Laplace transformation to the first row of (2), we can obtain

$$s^2 X(s) - sx_0 - v_{x0} = \omega_n^2 X(s) - \omega_n^2 P(s)$$

$$X(s) = \frac{s}{s^2 - \omega_n^2} x_0 + \frac{1}{s^2 - \omega_n^2} v_{x0} - \frac{\omega_n^2}{s^2 - \omega_n^2} P(s) \tag{3}$$

where x_0 and v_{x0} denote the initial position and initial velocity of the CoM in the sagittal plane, respectively. $P(s)$ denotes the Laplace transform of the sagittal ZMP trajectory $p(t)$. Then, applying inverse Laplace transformation, the sagittal CoM trajectory $x(t)$ can be obtained as

$$x(t) = x_0 \cosh(\omega_n t) + \frac{v_{x0}}{\omega_n} \sinh(\omega_n t) + \mathcal{L}^{-1}\left(\frac{-\omega_n^2}{s^2 - \omega_n^2} P(s)\right) \tag{4}$$

where $\mathcal{L}^{-1}(\cdot)$ denotes inverse Laplace transform.

Furthermore, the sagittal CoM velocity $v_x(t)$ can be obtained as the first derivative of (4):

$$v_x(t) = x_0 \omega_n \sinh(\omega_n t) + v_{x0} \cosh(\omega_n t) + \frac{d}{dt} \mathcal{L}^{-1}\left(\frac{-\omega_n^2}{s^2 - \omega_n^2} P(s)\right) \tag{5}$$

Since the lateral CoM trajectory $y(t)$ and the lateral CoM velocity $v_y(t)$ can be obtained in the same way, the dynamics of CoM in the sagittal and lateral planes can be expressed as follows:

$$\begin{bmatrix} x(t) \\ v_x(t) \end{bmatrix} = \begin{bmatrix} C(t) & \frac{1}{\omega_n} S(t) \\ \omega_n S(t) & C(t) \end{bmatrix} \begin{bmatrix} x_0 \\ v_{x0} \end{bmatrix} + \begin{bmatrix} \bar{p}(t) \\ \frac{d}{dt} \bar{p}(t) \end{bmatrix} \tag{6}$$

$$\begin{bmatrix} y(t) \\ v_y(t) \end{bmatrix} = \begin{bmatrix} C(t) & \frac{1}{\omega_n} S(t) \\ \omega_n S(t) & C(t) \end{bmatrix} \begin{bmatrix} y_0 \\ v_{y0} \end{bmatrix} + \begin{bmatrix} \bar{q}(t) \\ \frac{d}{dt} \bar{q}(t) \end{bmatrix} \tag{7}$$

with

$$\bar{p}(t) = \mathcal{L}^{-1}\left(\frac{-\omega_n^2}{s^2 - \omega_n^2} P(s)\right) \text{ and } \bar{q}(t) = \mathcal{L}^{-1}\left(\frac{-\omega_n^2}{s^2 - \omega_n^2} Q(s)\right)$$

where y_0 and v_{y0} denote the initial position and initial velocity of the CoM in the lateral plane, respectively. $C(t)$ and $S(t)$ are defined as $\cosh(\omega_n t)$ and $\sinh(\omega_n t)$, respectively. $Q(s)$ denotes Laplace transform of the lateral ZMP trajectory $q(t)$. It can be seen in (6) and (7) that the first term of the right-hand side is due to the initial conditions, and the second term is due to the given ZMP references.

2.2 Different types of ZMP

To generate a different type of motion it is necessary to utilize different types of ZMP references. In this paper, five types of ZMP components are considered, which are step function type, ramp function type, parabolic function type, cubic function type, and sine function type. In order to use these

different types of ZMP components, it is necessary to know the corresponding $\bar{p}(t)$ and $\bar{q}(t)$ of these components.

2.2.1 Step function type ZMP

Considering a step function type ZMP $p_{\text{step}}(t, A_s, T_s) = A_s u(t - T_s)$, where $u(\cdot)$ is the unit step function, its Laplace transform is

$$P_{\text{step}}(s) = \frac{A_s}{s} e^{-sT_s} \tag{8}$$

Multiplying by $-\omega_n^2 / (s^2 - \omega_n^2)$ and applying inverse Laplace transformation, the second term of its corresponding CoM trajectory $\bar{p}_{\text{step}}$ can be obtained as follows:

$$\bar{p}_{\text{step}}(t, A_s, T_s) = \mathcal{L}^{-1}\left(\frac{-\omega_n^2}{s^2 - \omega_n^2} \cdot \frac{A_s}{s} e^{-sT_s}\right) = \mathcal{L}^{-1}\left(A_s\left[\frac{1}{s} - \frac{s}{s^2 - \omega_n^2}\right] e^{-sT_s}\right)$$
$$= A_s[1 - \cosh(\omega_n(t - T_s))]u(t - T_s) \tag{9}$$

2.2.2 Ramp function type ZMP

Considering a ramp function type ZMP $p_{\text{ramp}}(t, A_r, T_r) = A_r t u(t - T_r)$, its Laplace transform is

$$P_{\text{ramp}}(s) = \frac{A_r}{s^2}(sT_r + 1)e^{-sT_r} \tag{10}$$

Similarly, the second term of its corresponding CoM trajectory $\bar{p}_{\text{ramp}}$ can be obtained as follows:

$$\bar{p}_{\text{ramp}}(t, A_r, T_r) = A_r\left[t - T_r\cosh(\omega_n(t - T_r)) - \frac{1}{\omega_n}\sinh(\omega_n(t - T_r))\right]u(t - T_r) \tag{11}$$

2.2.3 Parabolic function type ZMP

Considering a parabolic function type ZMP $p_{\text{para}}(t, A_p, T_p) = A_p t^2 u(t - T_p)$, its Laplace transform is

$$P_{\text{para}}(s) = A_p\left(\frac{T_p^2}{s} + \frac{2T_p}{s^2} + \frac{2}{s^3}\right)e^{-sT_p} \tag{12}$$

Similarly, the second term of its corresponding CoM trajectory $\bar{p}_{\text{para}}$ can be obtained as follows:

$$\bar{p}_{\text{para}}(t, A_p, T_p) = A_p\left[t^2 + \frac{2}{\omega_n^2} - \left(T_p^2 + \frac{2}{\omega_n^2}\right)\cosh(\omega_n(t - T_p)) - \frac{2T_p}{\omega_n}\sinh(\omega_n(t - T_p))\right]u(t - T_p) \tag{13}$$

2.2.4 Cubic function type ZMP

Considering a cubic function type ZMP $p_{\text{cubic}}(t, A_c, T_c) = A_c t^3 u(t - T_c)$, its Laplace transform is

$$P_{\text{cubic}}(s) = A_c\left(\frac{T_c^3}{s} + \frac{3T_c^2}{s^2} + \frac{6T_c}{s^3} + \frac{6}{s^4}\right)e^{-sT_c} \tag{14}$$

Similarly, the second term of its corresponding CoM trajectory $\bar{p}_{\text{cubic}}$ can be obtained as follows:

$$\bar{p}_{\text{cubic}}(t, A_c, T_c) = A_c\left[t^3 + \frac{6}{\omega_n^2}t + 2T_c^3 - \left(T_c^3 + \frac{6T_c}{\omega_n^2}\right)\cosh(\omega_n(t - T_c))\right.$$
$$\left. - \left(\frac{3T_c^2}{\omega_n} + \frac{6}{\omega_n^3}\right)\sinh(\omega_n(t - T_c))\right]u(t - T_c) \tag{15}$$

2.2.5 Sine function type ZMP

Considering a sine function type ZMP $p_{\sin}(t, A_\beta, \alpha, T_\beta) = A_\beta \sin(\alpha t)u(t - T_\beta)$, its Laplace transform is

$$P_{\sin}(s) = (\phi_s s + \psi_s)\frac{e^{-sT_\beta}}{s^2 + \alpha^2} \tag{16}$$

where $\phi_s = A_\beta \sin(\alpha T_\beta)$ and $\psi_s = \alpha A_\beta \cos(\alpha T_\beta)$.

Similarly, the second term of its corresponding CoM trajectory $\overline{p}_{\sin}$ can be obtained as follows:

$$\overline{p}_{\sin}(t, A_\beta, \alpha, T_\beta) = \frac{1}{\alpha^2 + \omega_n^2} \left[\phi_s \omega_n^2 \cos(\alpha(t - T_\beta)) + \frac{\psi_s}{\alpha} \omega_n^2 \sin(\alpha(t - T_\beta)) \right.$$
$$\left. - \phi_s \omega_n^2 \cosh(\omega_n(t - T_\beta)) - \psi_s \omega_n \sinh(\omega_n(t - T_\beta)) \right] u(t - T_\beta) \tag{17}$$

In addition, for a cosine function type ZMP $p_{\cos}(t, A_\beta, a, T_\beta) = A_\beta \cos(\alpha t) u(t - T_\beta)$, the second term of its corresponding CoM trajectory $\overline{p}_{\cos}$ is

$$\overline{p}_{\cos}(t, A_\beta, \alpha, T_\beta) = \frac{1}{\alpha^2 + \omega_n^2} \left[\phi_c \omega_n^2 \cos(\alpha(t - T_\beta)) + \frac{\psi_c}{\alpha} \omega_n^2 \sin(\alpha(t - T_\beta)) \right.$$
$$\left. - \phi_c \omega_n^2 \cosh(\omega_n(t - T_\beta)) - \psi_c \omega_n \sinh(\omega_n(t - T_\beta)) \right] u(t - T_\beta) \tag{18}$$

where $\phi_c = A_\beta \cos \alpha T_\beta$ and $\psi_c = -\alpha A_\beta \sin \alpha T_\beta$.

2.3 Center of mass trajectory generation by given ZMP references

So far, by being given a suitable ZMP reference and suitable initial conditions, the CoM trajectory can be acquired with (6) and (7). However, there is a problem when using (6) and (7) to calculate the CoM trajectory since there are cosh term and sinh term in (6) and (7). The value of cosh term and sinh term tend to infinity as t becomes much greater than 0. Hence, a complete gait pattern is divided into several partitions according to the number of steps, and the CoM trajectory is generated step by step with given boundary conditions for each step. Hereafter, the CoM trajectory will be discussed for a single step.

2.3.1 Common ZMP reference
Generally, the most common ZMP reference for a single step is defined as follows:

$$\begin{cases} p_n(t) = A_n u(t) \\ q_n(t) = B_n u(t) \end{cases} \text{ for } t \in (0, T] \tag{19}$$

where T denotes the period of a step, which is half of the walking period. Subscript n denotes the nth step. A_n and B_n denote sagittal amplitude and lateral amplitude of ZMP for the nth step. Since the following discusses the CoM trajectory of a single step as well, the subscript n will be omitted for simplicity when there is no ambiguity.

2.3.2 Double support phase ZMP reference
It is obvious that the common ZMP reference does not consider DSP. On the other hand, a ZMP reference taking into account DSP can be expressed as follows:

$$\begin{cases} p^{\mathrm{D}}(t) = \left(A - d_1 + \frac{d_1}{k_v T} t\right)[u(t) - u(t - t_1)] + A[u(t - t_1) - u(t - t_2)] + \left[A + \frac{d_2}{k_v T}(t - t_2)\right]u(t - t_2) \\ q^{\mathrm{D}}(t) = \left(q_0 + \frac{B - q_0}{k_v T} t\right)[u(t) - u(t - t_1)] + B[u(t - t_1) - u(t - t_2)] + \left[B + \frac{q_f - B}{k_v T}(t - t_2)\right]u(t - t_2) \end{cases} \tag{20}$$

where $A - d_1$ and $A + d_2$ are initial and final positions of p, respectively, and q_0 and q_f are initial and final positions of q, respectively. It is noted that when walking in a straight line, the values of q_0 and q_f are usually set as 0, namely $q_0 = q_f = 0$. A, B and the initial and final positions of p and q are user-defined parameters for designing a desired ZMP reference, and these parameters are determined by a parameterized gait planning algorithm in this paper, which will be examined in Section 3. Superscript D denotes the ZMP reference taking into account DSP, k_v denotes virtual DSP scale, t_1 is $k_v T$, and t_2 is $(1 - k_v T)$. As shown in Figure 2, the DSP-ZMP reference is composed of three intervals. The first interval is a DSP whose range is $(0, t_1]$. The second phase is an SSP whose range is $(t_1, t_2]$. The third interval is a DSP whose range is $(t_2, T]$. ZMP moves within the DSP and stays at a fixed point within the SSP. In addition, d_1 and d_2 denote the incremental amount of sagittal amplitude within the first interval and the third interval, respectively. It is important that d_1 and d_2 should be positive since the gait pattern is generated for walking forward.
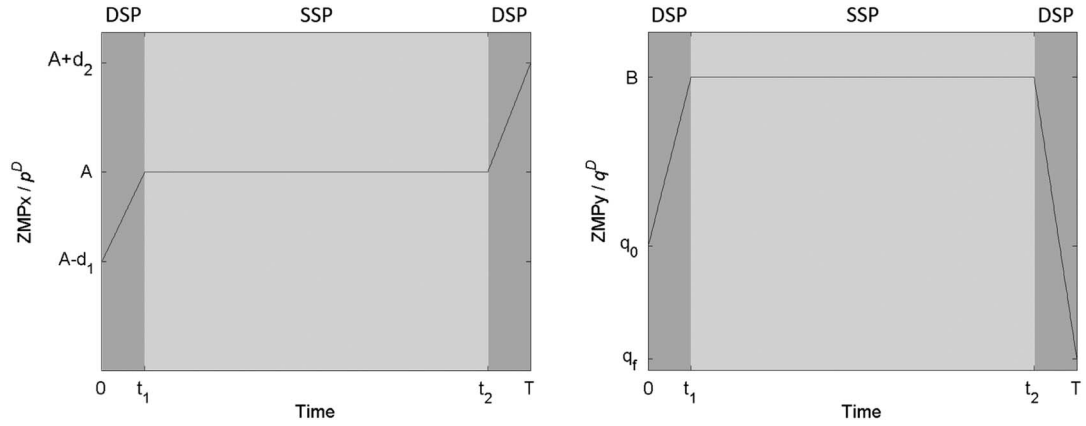
Figure 2 DSP-ZMP reference. SSP = single support phase; DSP = double support phase

2.3.3 Moving ZMP reference

In human walking, ZMP moves continuously even during SSP. Thus, Erbatur and Kurt (2009) defined a ZMP reference with ZMP moving forward slightly during SSP as a natural ZMP reference. Inspired by this concept, we define a moving ZMP reference as follows:

$$
\begin{cases}
p^{\mathrm{M}}(t) = \left(A - d_1 + \frac{d_1 - a}{k_v T} t\right)[u(t) - u(t - t_1)] + \left[A - a + \frac{2a}{(1 - 2k_v)T}(t - t_1)\right][u(t - t_1) - u(t - t_2)] \\
\qquad + \left[A + a + \frac{d_2 - a}{k_v T}(t - t_2)\right] u(t - t_2) \\
q^{\mathrm{M}}(t) = \left(q_0 + \frac{B - q_0}{k_v T} t\right)[u(t) - u(t - t_1)] + \left[B + b\sin\left(\frac{\pi}{(1 - 2k_v)T}(t - t_1)\right)\right][u(t - t_1) - u(t - t_2)] \\
\qquad + \left[B + \frac{q_f - B}{k_v T}(t - t_2)\right] u(t - t_2)
\end{cases}
\tag{21}
$$

where a denotes half of the distance that ZMP moves forward during an SSP, and b denotes the incremental amount of lateral amplitude during an SSP. It is noted that B and b must have the same sign. In addition, the DSP-ZMP reference is a special case of a moving ZMP reference while $a = 0$ and $b = 0$.

With the proposed moving ZMP reference, the ZMP can move during SSP not only in the sagittal plane but also in the lateral plane, which makes the robot walk more naturally and in a more human-like way. To obtain the corresponding CoM trajectory of the moving ZMP reference, (21) can be rewritten as follows:

$$
\begin{cases}
p^{\mathrm{M}}(t) = (L_{p1} + K_{p1}t)[u(t) - u(t - t_1)] + (L_{p2} + K_{p2}t)[u(t - t_1) - u(t - t_2)] \\
\qquad + (L_{p3} + K_{p3}t)u(t - t_2) \\
q^{\mathrm{M}}(t) = (L_{q1} + K_{q1}t)[u(t) - u(t - t_1)] + \left[L_{q2} + K_{q2}\sin(\alpha t - t_d)\right][u(t - t_1) - u(t - t_2)] \\
\qquad + (L_{q3} + K_{q3}t)u(t - t_2)
\end{cases}
\tag{22}
$$

with

$$
L_{p1} = A - d_1,\ L_{p2} = A - a - \frac{2at_1}{(1 - 2k_v)T},\ L_{p3} = A + a - \frac{(d_2 - a)t_2}{k_v T}
$$

$$
K_{p1} = \frac{d_1 - a}{k_v T},\ K_{p2} = \frac{2a}{(1 - 2k_v)T},\ K_{p3} = \frac{d_2 - a}{k_v T}
$$

$$
L_{q1} = q_0,\ L_{q2} = B,\ L_{q3} = B - \frac{(q_f - B)t_2}{k_v T}
$$

$$
K_{q1} = \frac{B - q_0}{k_v T},\ K_{q2} = b,\ K_{q3} = \frac{q_f - B}{k_v T},\ \alpha = \frac{\pi}{(1 - 2k_v)T},\ t_d = \alpha t_1
$$

Since $p^M(t)$ and $q^M(t)$ are linear combinations of step, ramp, and sine function type ZMP, $\overline{p}^M(t)$ and $\overline{q}^M(t)$ of the moving ZMP reference can be obtained using (9), (11), (17), and (18) as follows:

$$\overline{p}^M(t) = \overline{p}_{\text{step}}(t, L_{p1}, 0) + \overline{p}_{\text{ramp}}(t, K_{p1}, 0) + \overline{p}_{\text{step}}(t, L_{p2} - L_{p1}, t_1) + \overline{p}_{\text{ramp}}(t, K_{p2} - K_{p1}, t_1)$$
$$+ \overline{p}_{\text{step}}(t, L_{p3} - L_{p2}, t_2) + \overline{p}_{\text{ramp}}(t, K_{p3} - K_{p2}, t_2) \tag{23}$$

$$\overline{q}^D(t) = \overline{p}_{\text{step}}(t, L_{q1}, 0) + \overline{p}_{\text{ramp}}(t, K_{q1}, 0) + \overline{p}_{\text{step}}(t, L_{q2} - L_{q1}, t_1) + \overline{p}_{\text{ramp}}(t, -K_{q1}, t_1)$$
$$+ \cos(t_d)\overline{p}_{\text{sin}}(t, K_{q2}, \alpha, t_1) - \sin(t_d)\overline{p}_{\cos}(t, K_{q2}, \alpha, t_1)$$
$$+ \overline{p}_{\text{step}}(t, L_{q3} - L_{q2}, t_2) + \overline{p}_{\text{ramp}}(t, K_{q3}, t_2) - \cos(t_d)\overline{p}_{\sin}(t, K_{q2}, \alpha, t_2) + \sin(t_d)\overline{p}_{\cos}(t, K_{q2}, \alpha, t_2) \tag{24}$$

So far, the corresponding CoM trajectory of the moving reference can be obtained by substituting (23) and (24) into (6) and (7), respectively. However, the initial conditions of the DSP-ZMP reference are still unknown. To determine the initial conditions, we define the boundary conditions of the CoM trajectory as initial and final positions of ZMP, namely $x_0^M = p^M(0) = A - d_1$, $x^M(T) = p^M(T) = A + d_2$, $y_0^M = q^M(0) = q_0$, and $y^M(T) = q^M(T) = q_f$. Then, substituting these boundary conditions into the first row of (6) and (7), the initial velocity of a moving reference can be obtained as

$$\begin{cases} v_{x0}^M = \frac{\omega_n}{S(T)}\left[x^M(T) - C(T)x_0^M - \overline{p}^M(T)\right] = \frac{\omega_n}{S(T)}\left[A + d_2 - C(T)(A - d_1) - \overline{p}^M(T)\right] \\ v_{y0}^M = \frac{\omega_n}{S(T)}\left[y^M(T) - C(T)y_0^M - \overline{q}^M(T)\right] = \frac{\omega_n}{S(T)}\left[q_f - C(T)q_0 - \overline{q}^M(T)\right] \end{cases} \tag{25}$$
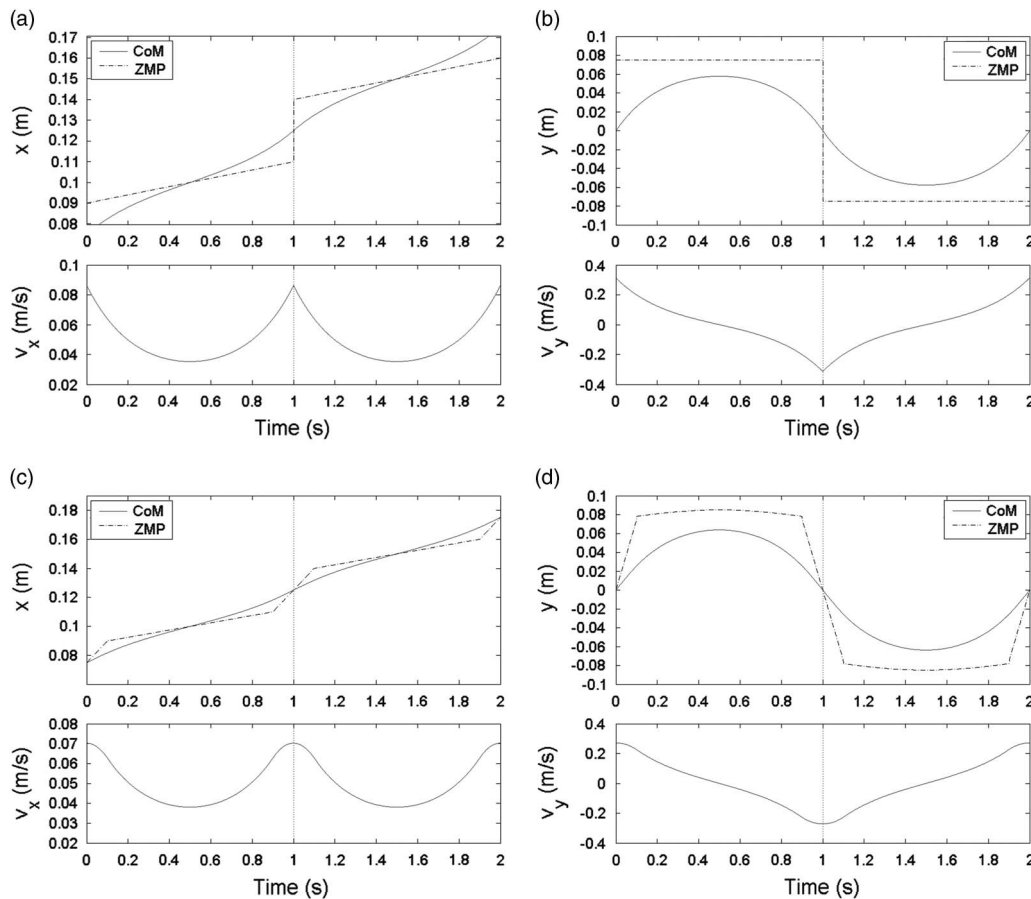

Figure 3 Corresponding center of mass (CoM) trajectories of moving ZMP references without double support phase (DSP) and with DSP. In the top of (a) and (c), the solid line and the dashed line denote the CoM trajectory and ZMP trajectory in x-axis, respectively. In the bottom of (a) and (c), v_x denotes velocity of CoM in x-axis. Similarly, in the top of (b) and (d), the solid line and the dashed line denote the CoM trajectory and ZMP trajectory in y-axis, respectively. In the bottom of (b) and (d), v_y denotes velocity of CoM in y-axis.

Figure 3 shows a moving ZMP reference with two steps. A_1 and A_2 are 0.1 and 0.15, respectively. B_1 and B_2 are 0.075 and -0.075, respectively. d_1 and d_2 of both steps are set as 0.025, and q_0 and q_f of both steps are set as 0. a of both steps are set as 0.01. b_1 and b_2 are set as 0.01 and -0.01, respectively. T and z_c are set as 1 second and 0.52975 m, respectively. Figure 3(a, b) shows CoM trajectories of the moving ZMP reference without DSP. Figure 3(c, d) shows CoM trajectories of the moving ZMP reference with DSP, and k_v is set as 0.1. It can be seen that at the boundary ($T = 1$ second), the velocity of the moving ZMP reference with DSP is smoother than that of the moving ZMP reference without DSP. Velocity smoothness means the velocity is continuous derivative at boundaries. Hence, the ZMP reference with DSP is more reliable because of its smooth transition.

3 Parameterized gait planning algorithm

In Section 2.3, a CoM trajectory with the moving ZMP reference has been introduced. In order to generate a complete gait pattern using the proposed CoM trajectory with desired footprint location, a parameterized gait planning algorithm is presented in this section. Once the user-defined parameters are determined, the initial conditions and CoM trajectory for each step can be obtained and the overall gait pattern can be acquired using the gait planning algorithm. The gait planning algorithm consists of the following steps:

i.   Determine the user-defined parameters including step period T, step height H, step width W, number of steps N, virtual DSP ratio k_v, and DSP ratio k. It is noted that the period of DSP is defined by k instead of k_v. The period of DSP T_{DSP} is $2kT$ and the period of SSP T_{SSP} is $(1-2k)T$. The range of k is set as $(0, 0.25]$ so that T_{DSP} will not be greater than half of the period T and there is sufficient time for the swing leg to step forward. k_v is used to tune the boundary velocities for a smooth transition between steps.

ii. Determine the step size of each step S_n for $n \in \{1, 2, \ldots, N\}$, and it is important that S_N should be 0 so that the walking distances of both legs can be identical. Then, as in the footprint definition shown in Figure 4, stride length L_n can be obtained as $L_n = S_n + S_{n-1}$ for $n \in \{1, 2, \ldots, N\}$ with $S_0 = 0$. Furthermore, assuming the first swing leg is the right leg of the robot, the stride length of a specific leg for each step is defined as follows:

$$L_{r,n} = \begin{cases} L_n, & \text{for } n = \{2i-1 \mid \forall i \in N^+,\ 2i-1 \leqslant N\} \\ 0, & \text{for } n = \{2i \mid \forall i \in N^+,\ 2i \leqslant N\} \end{cases} \tag{26}$$

$$L_{l,n} = \begin{cases} 0, & \text{for } n = \{2i-1 \mid \forall i \in N^+,\ 2i-1 \leqslant N\} \\ L_n, & \text{for } n = \{2i \mid \forall i \in N^+,\ 2i \leqslant N\} \end{cases} \tag{27}$$

where $L_{r,n}$ and $L_{l,n}$ denote the stride length of the right and left legs for the nth step, respectively. For example, if the robot takes four steps and $S = [0.05, 0.05, 0.05, 0]$, then $L_r = [0.05, 0, 0.1, 0]$ and $L_l = [0, 0.1, 0, 0.05]$.

iii. Calculate the sagittal amplitude of each step, namely A_n for $n \in \{1, 2, \ldots, N\}$. A_n is defined as

$$A_n = L_{n-1} + A_{n-2} \text{ for } n \in \{2, \ldots, N\} \tag{28}$$

with $A_0 = 0$ and $A_1 = 0$. It is noted that A_0 is just a virtual sagittal amplitude for calculating A_n and is not used in the following steps. A_1 is defined as 0 so that the robot can walk with zero initial velocity.

iv. Determine B_n, a_n, and b_n for each step. Generally, if step width W is identical for all steps, then B_n can be defined as

$$B_n = (-1)^{n-1} W \big/ 2 \text{ for } n \in \{1, \ldots, N\} \tag{29}$$

a_n and b_n should be relatively small values to A_n and B_n, respectively.
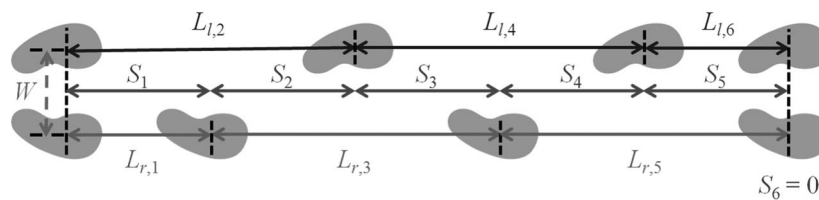

Figure 4 Definitions of step size and stride length for footprint location

v. Calculate the boundary conditions for each step, namely $A_n - d_{1,n}$, $A_n + d_{2,n}$, $q_{0,n}$, and $q_{f,n}$ for $n \in \{1, 2, \ldots, N\}$. In order to accelerate from zero initial velocity at the first step and decelerate to zero final velocity at the final step in the sagittal plane, $d_{1,1}$ and $d_{2,N}$ are set as 0. d_2 of the other steps are defined as follows:

$$d_{2,n} = \frac{A_{n+1} - A_n}{2} \text{ for } n \in \{1, \ldots, N-1\} \tag{30}$$

In addition, since the initial position of a step must be the same as the final position of its previous step, we can know

$$d_{1,n+1} = d_{2,n} \text{ for } n \in \{1, \ldots, N-1\} \tag{31}$$

Similarly, $q_{0,1}$ and $q_{f,N}$ are set as 0, and q_0 and q_f of the other step are defined as

$$q_{f,n} = \frac{B_{n+1} + B_n}{2} \text{ for } n \in \{1, \ldots, N-1\} \tag{32}$$

$$q_{0,n+1} = q_{f,n} \text{ for } n \in \{1, \ldots, N-1\} \tag{33}$$

vi. Calculate the initial position and the initial velocity for each step with (25).

vii. Calculate the CoM trajectory step by step with (6) and (7).

viii. Concatenate the CoM trajectories of all steps together to obtain the complete CoM trajectory as follows

$$x(t) = \sum_{n=1}^{N} x_n(t - (n-1)T)[u(t - (n-1)T) - u(t - nT)] \tag{34}$$

$$y(t) = \sum_{n=1}^{N} y_n(t - (n-1)T)[u(t - (n-1)T) - u(t - nT)] \tag{35}$$

ix. Calculate the foot trajectories with respect to the world coordinate system. The foot trajectory generation is divided into two parts. Swing foot trajectory is obtained using a rolling cycle (Liu *et al.*, 2013), and the supporting foot trajectory stays at a fixed point. Thus, the foot trajectories for nth step are defined as

$$footx_{j,n}(t) = \begin{cases} 0, & \text{if } t \leqslant t_1 \\ \frac{L_{j,n}}{2\pi}(\theta - \sin\theta), & \text{if } t_1 < t \leqslant t_2 \\ L_{j,n}, & \text{otherwise} \end{cases} \tag{36}$$

$$footy_{l,n}(t) = \frac{1}{2}W \text{ and } footy_{r,n}(t) = -\frac{1}{2}W \tag{37}$$

$$footz_{j,n}(t) = \begin{cases} \frac{H}{2}(1 - \cos\theta), & \text{if } t_1 < t \leqslant t_2 \\ 0, & \text{otherwise} \end{cases} \tag{38}$$

where $t_1 = kT$, $t_2 = (1-k)T$, $\theta = 2\pi(t - t_1)/(t_2 - t_1)$, and $t \in (0,T]$. $j \in \{r, l\}$, r and l denote the right foot and the left foot, respectively. Then, a complete foot trajectory with respect to the world coordinate system can be obtained as follows:

$$footx_j(t) = \sum_{n=1}^{N} [O_{j,n} + footx_{j,n}(t - (n-1)T)][u(t - (n-1)T) - u(t - nT)] \tag{39}$$

$$footy_l(t) = \frac{1}{2}W \text{ and } footy_r(t) = -\frac{1}{2}W \tag{40}$$

$$footz_j = \sum_{n=1}^{N} footz_{j,n}(t - (n-1)T)[u(t - (n-1)T) - u(t - nT)] \tag{41}$$

with $O_{j,1} = 0$, $O_{j,n} = \sum_{m=1}^{n-1} L_{j,m}$ for $n \in \{2, \ldots, N\}$ and $j \in \{r, l\}$.

x. Finally, calculate the foot trajectories with respect to the joint coordinate system and apply inverse kinematics.

4 Experiments

Parameterized gait patterns have been generated for the teen-sized humanoid robot, David Junior, which is 96 cm tall and weighs about 9.4 kg. The CoM height z_c of David is 52.975 cm. David has 26 d.f. as shown in Figure 5. Each leg consists of 6 d.f. and weighs 2.177 kg. Each arm consists of 5 d.f., and the mass of the upper body with arms is 4.96 kg.

The gait patterns consist of eight steps (four walking cycles), namely $N = 8$. The first swing leg is assigned the right leg. The step period T was set as 0.85 seconds and DSP ratio k was set as 0.22. Thus, DSP period T_{DSP} was 0.374 seconds and SSP period T_{SSP} was 0.476 seconds. The magnitude of the lateral amplitude was set as 8 cm, so $B = [8, -8, 8, -8, 8, -8, 8, -8]$ cm. a_n for all steps were set as 0.5 cm. b was set as $[0.5, -0.5, 0.5, -0.5, 0.5, -0.5, 0.5, -0.5]$ cm. Virtual DSP ratio k_v was set as 0.1. To demonstrate the feasibility of the proposed method, two different gait patterns were generated with different step size S. Step height H was set as 3 cm.

In the first gait pattern, each step size was set as 5 cm except the final step, namely $S = [5, 5, 5, 5, 5, 5, 5, 0]$ cm. Figures 6 and 7 show the sagittal and lateral trajectory of CoM, respectively. Figure 8 shows foot trajectories with respect to X-axis and Z-axis. Figure 9 shows the ZMP reference and the CoM trajectory of the first gait pattern in XY plane. Foot trajectories of both legs depicted with plus sign markers are also shown in Figure 9.

In the second gait pattern, S was set as $[2, 2, 3, 4, 5, 4, 3, 0]$ cm. The lateral CoM trajectory of the second gait pattern was set the same as in the first gait pattern, and the sagittal CoM trajectory is shown in Figure 10. Foot trajectories with respect to the X-axis are shown in Figure 11. Figure 12 shows the ZMP reference, CoM trajectory, and foot trajectories of both legs in the XY plane.

To verify that the moving ZMP reference with DSP is more reliable than the moving ZMP reference without DSP, a simulation study was carried out on Webots (Michel, 2004), which is a powerful robot simulator widely used in robotic research. Both of the gait patterns mentioned above were performed in the simulator, and actual ZMP trajectories were measured for verification. The robot model of the simulation was modeled based on the specification of David as shown in Figure 13. Although there is modeling error between the real robot and the simulation model, the simulation results are still reliable.

Four force sensors are equipped underneath the corners of each sole to measure actual ZMP trajectories. The measured ZMP trajectories of the first and the second gait pattern are shown in Figures 14 and 15, respectively. The solid lines denote the measured ZMP trajectory and the dotted lines denotes the boundaries of foot trajectory in Figures 14 and 15. It can be seen that the measured ZMP trajectory of the ZMP reference with DSP is more regular than that of the ZMP reference without DSP, and vibration of the former is also smaller. Furthermore, in Figures 14(a) and 15(a), it can be seen that overshoot occurs while support phase transitions. It is especially serious at the transitions marked with the red circles because ZMP almost exceeds the boundary of the support polygon. Therefore, the reliability of the moving ZMP reference with DSP can be verified with this simulation.

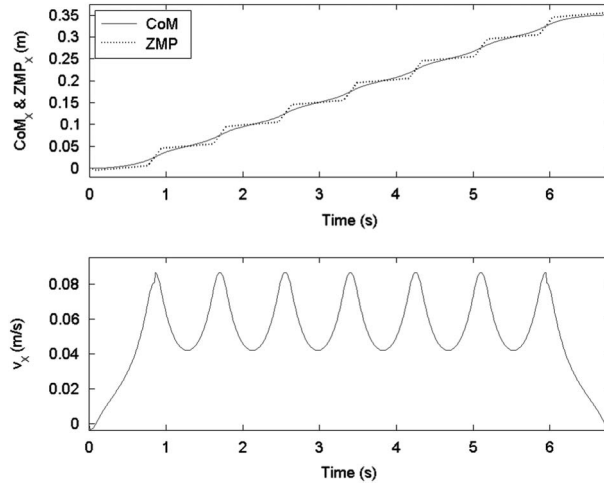**Figure 5**   Teen-sized humanoid robot, David Junior

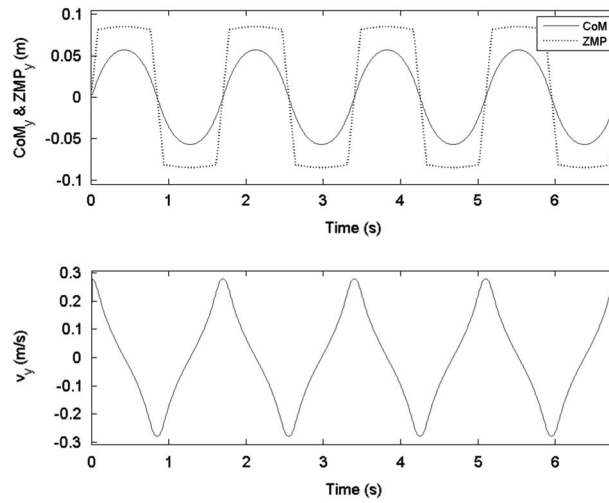**Figure 6** ZMP reference and center of mass (CoM) trajectory in the sagittal plane for the first gait pattern

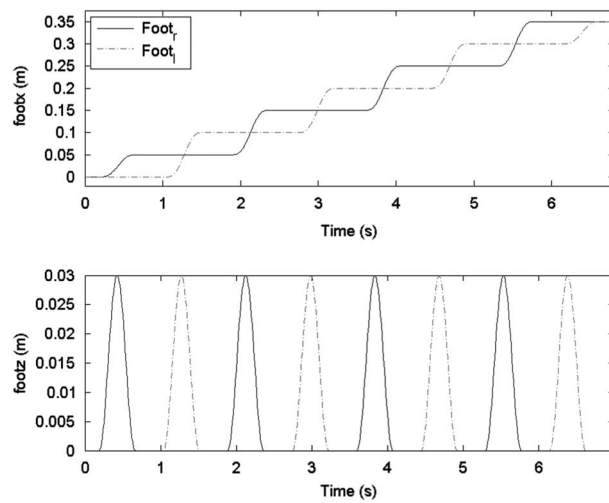**Figure 7** ZMP reference and center of mass (CoM) trajectory in the lateral plane

Figure 8 Foot trajectories for the first gait pattern
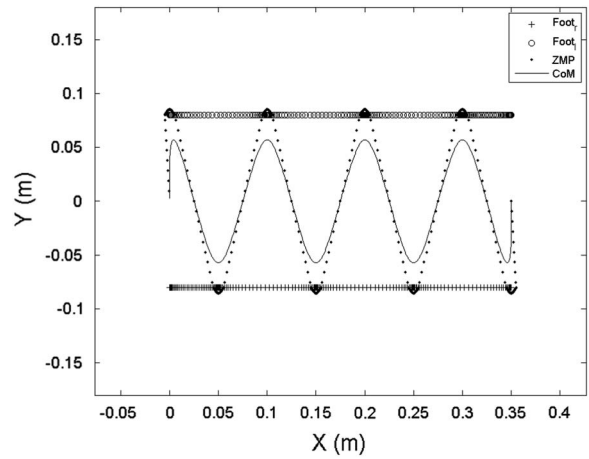
Figure 9   ZMP reference and center of mass (CoM) trajectory in the XY plane for the first gait pattern
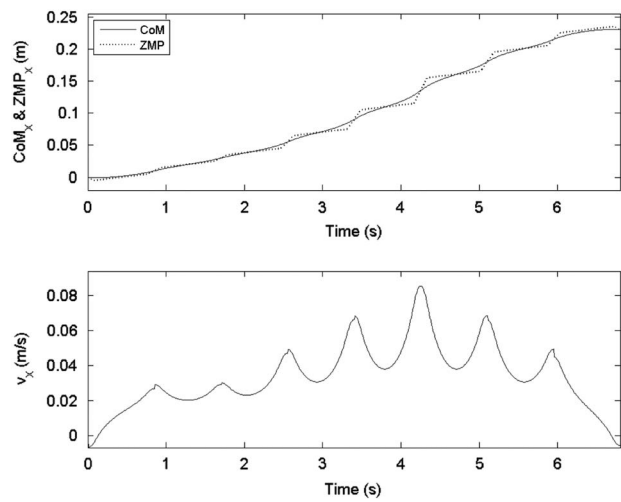

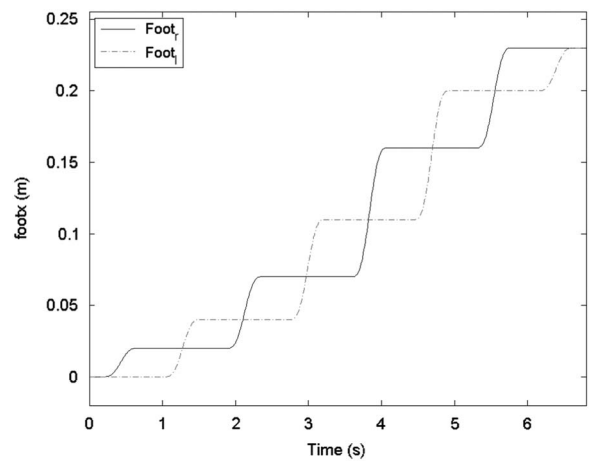**Figure 10**   ZMP reference and center of mass (CoM) trajectory in the sagittal plane for the second gait pattern

Figure 11   Foot trajectories with respect to the X-axis for the second gait pattern
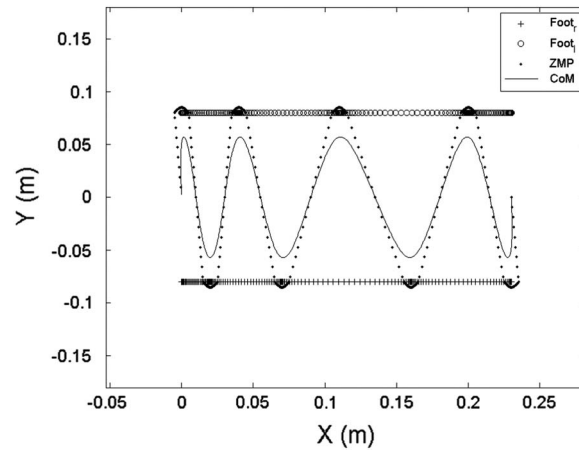
Figure 12 ZMP reference and center of mass (CoM) trajectory in the XY plane for the second gait pattern
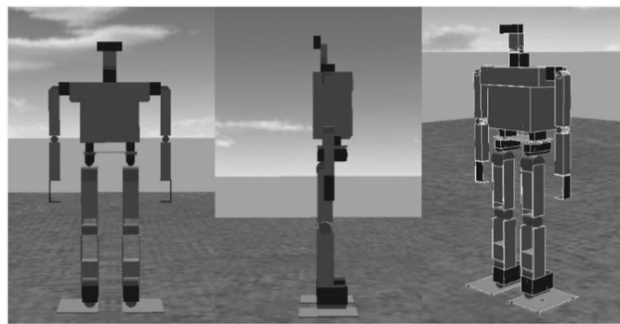

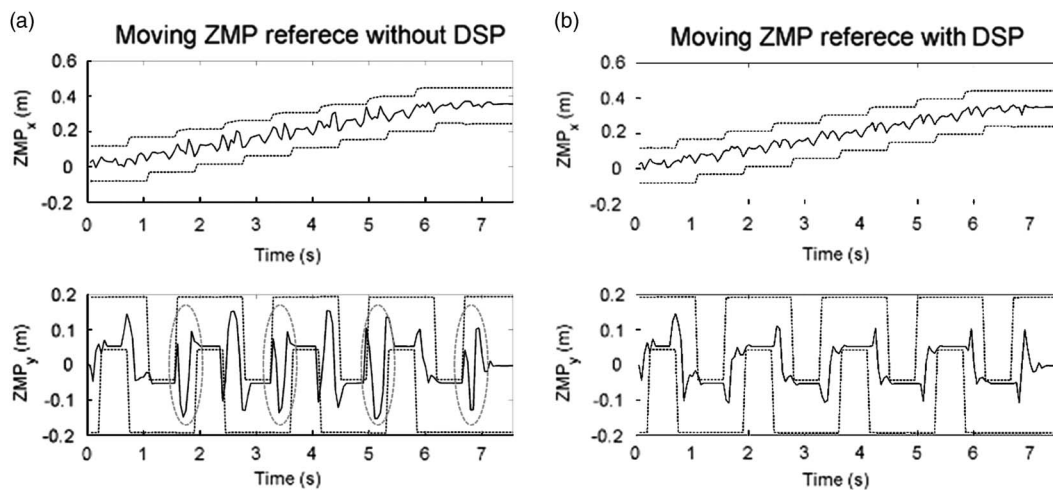**Figure 13** The model of David in the robot simulator

Figure 14 Measured ZMP trajectory of the first gait pattern. DSP = double support phase. ZMPx denotes the x coordinate of the ZMP, and ZMPy denotes the y coordinate of the ZMP

Eventually, gait patterns mentioned above were performed by David, and snapshots of both gait patterns are shown in Figure 16 (refer to the Supplementary Video 1) and Figure 17 (refer to the Supplementary Video 2), respectively. It can be seen that David Junior was able to walk stably
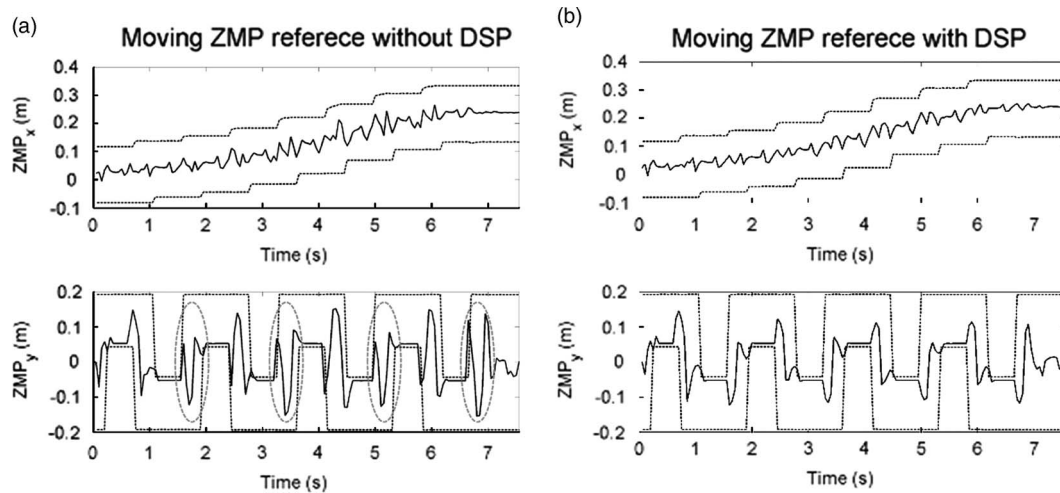
Figure 15 Measured ZMP trajectory of the second gait pattern. ZMPx denotes the x coordinate of the ZMP, and ZMPy denotes the y coordinate of the ZMP. DSP = double support phase

with both gait patterns generated by using the proposed method. In addition, with gait patterns generated by using the proposed method (refer to the Supplementary Video 3), David won first place in the HuroCup sprint event at the 20th Federation of International Robot-soccer Association (FIRA) RoboWorld Cup competition, which is a well-known international robotic competition held annually. Thus, the feasibility of the proposed method has been validated.

5 Conclusions

A parameterized gait pattern generator with a natural ZMP reference for biped walking has been proposed in this paper. Five types of ZMP components are presented for formulating the natural ZMP reference, and the corresponding terms for the CoM trajectory are also derived based on the relationship between ZMP and CoM from LIPM theory. Moreover, a gait planning algorithm is presented for generating a gait pattern with user-defined parameters so that parameterized gait pattern generation can be achieved. Finally, the simulation and experimental results validate the feasibility of the proposed method.

In this paper, the CoM trajectory is acquired based on a natural ZMP reference. Another factor to achieve natural walking or human-like walking may be heel-to-toe walking, which means the contact point transition of the supporting foot starts at heel-strike and ends at toe-off. Thus, extra sensors and feedback controller on the sole for achieving heel-to-toe walking can be considered as future works to enhance the walking stability and natural walking.

Acknowledgments

Supplementary material

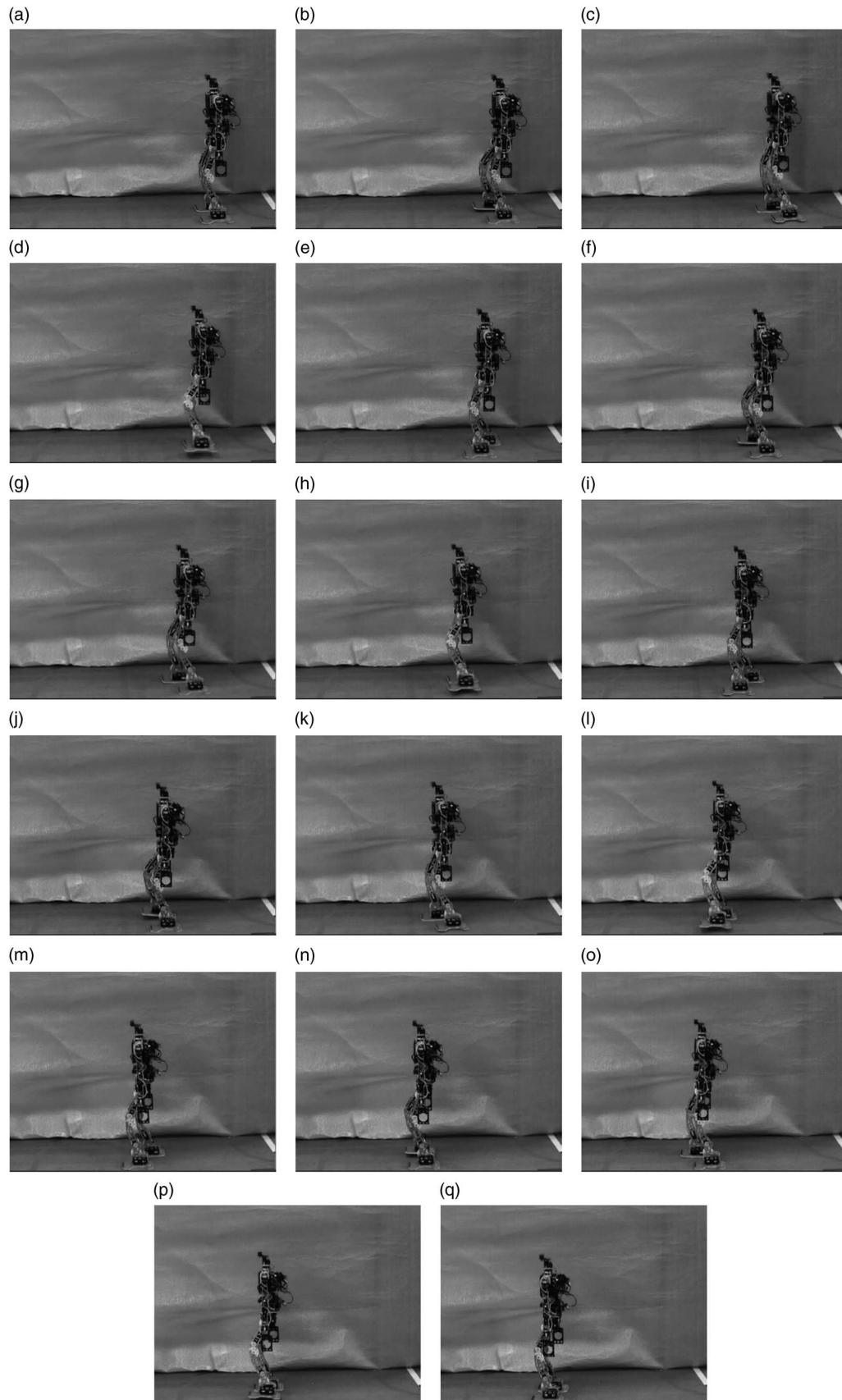To view supplementary material for this article, please visit http://dx.doi.org/10.1017/S0269888 916000138

Figure 16 Snapshots for the first gait pattern with $S = [5, 5, 5, 5, 5, 5, 5, 0]$ cm. The robot walks stably with identical step sizes

(a)
(b)
(c)

(d)
(e)
(f)

(g)
(h)
(i)

(j)
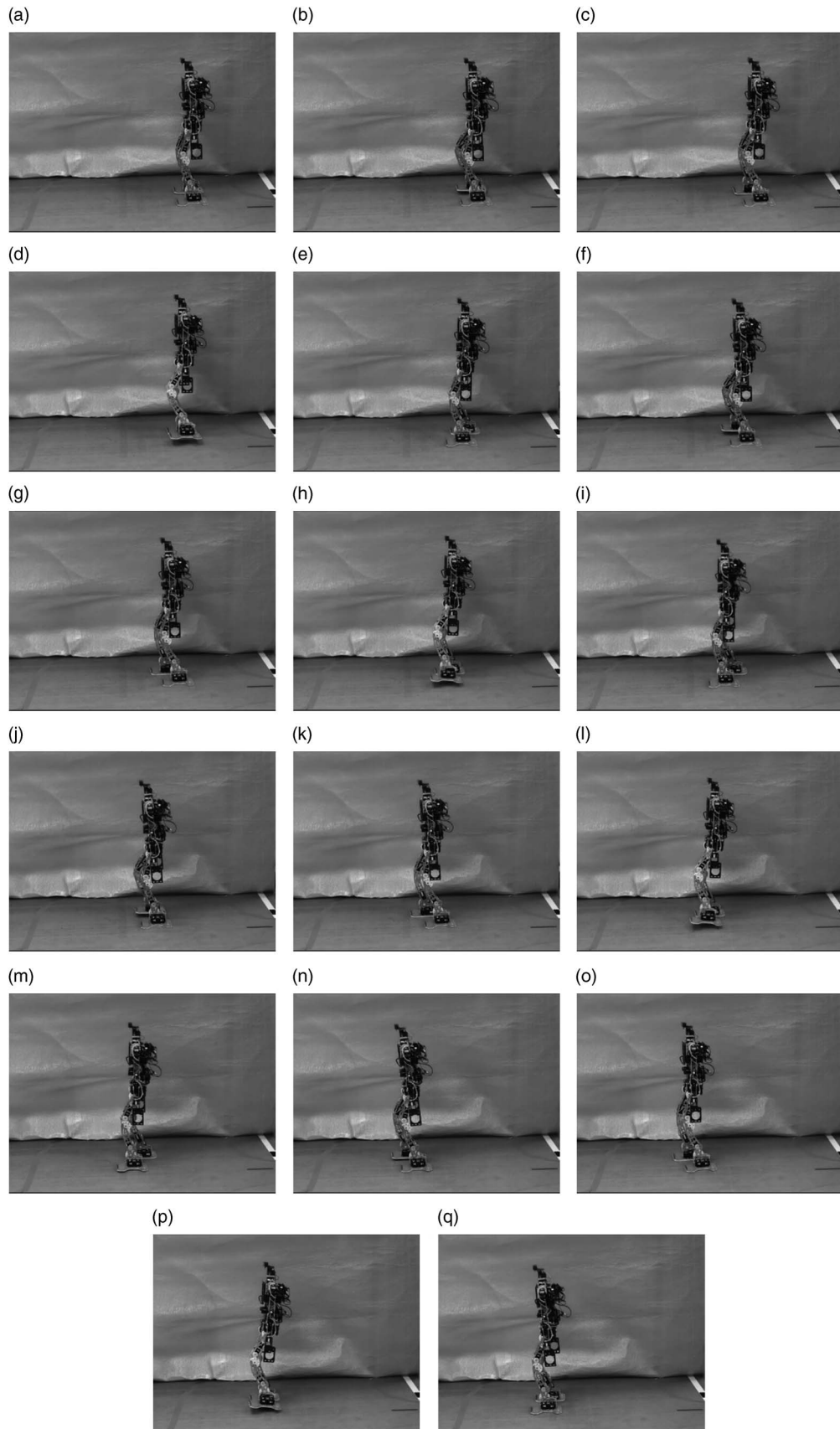(k)
(l)

(m)
(n)
(o)

(p)
(q)

Figure 17 Snapshots for the second gait pattern with $S = [2, 2, 3, 4, 5, 4, 3, 0]$ cm. The robot walks stably with different step sizes

References

Choi, Y., You, B. J. & Oh, S. R. 2004. On the stability of indirect ZMP controller for biped robot systems. In *Proceedings of 2004 IEEE/RSJ International Conference on Intelligent Robots and Systems*, **2**, 1966–1971.

Endo, G., Morimoto, J., Matsubara, T., Nakanishi, J. & Cheng, G. 2008. Learning CPG-based biped locomotion with a policy gradient method: application to a humanoid robot. *The International Journal of Robotics Research* **27**(2), 213–228.

Erbatur, K. & Kurt, O. 2009. Natural ZMP trajectories for biped robot reference generation. *IEEE Transactions on Industrial Electronics* **56**(3), 835–845.

Farzaneh, Y., Akbarzadeh, A. & Akbari, A. A. 2014. Online bio-inspired trajectory generation of seven-link biped robot based on T–S fuzzy system. *Applied Soft Computing* **14**, 167–180.

Ferreira, J. P., Crisóstomo, M. & Coimbra, A. P. 2011. Sagittal stability PD controllers for a biped robot using a neurofuzzy network and an SVR. *Robotica* **29**(5), 717–731.

Hu, L., Zhou, C. & Sun, Z. 2008. Estimating biped gait using spline-based probability distribution function with Q-learning. *IEEE Transactions on Industrial Electronics* **55**(3), 1444–1452.

Kajita, S., Kanehiro, F., Kaneko, K., Yokoi, K. & Hirukawa, H. 2001. The 3D linear inverted pendulum mode: a simple modeling for a biped walking pattern generation. In *Proceedings of 2001 IEEE/RSJ International Conference on Intelligent Robots and Systems*, **1**, 239–246.

Kajita, S., Morisawa, M., Harada, K., Kaneko, K., Kanehiro, F., Fujiwara, K. & Hirukawa, H. 2006. Biped walking pattern generator allowing auxiliary ZMP control. In *Proceedings of 2006 IEEE/RSJ International Conference on Intelligent Robots and Systems*, 2993–2999.

Kajita, S., Nagasaki, T., Kaneko, K. & Hirukawa, H. 2007. ZMP-based biped running control. *IEEE Robotics & Automation Magazine* **2**(14), 63–72.

Kim, D., Seo, S. J. & Park, G. T. 2005. Zero-moment point trajectory modelling of a biped walking robot using an adaptive neuro-fuzzy system. *IEE Proceedings – Control Theory and Applications* **152**(4), 411–426.

Li, T. H. S., Kuo, P. H., Ho, Y. F., Kao, M. C. & Tai, L. H. 2015. A biped gait learning algorithm for humanoid robots based on environmental impact assessed artificial bee colony. *IEEE Access* **3**, 13–26.

Li, T. H. S., Su, Y. T., Lai, S. W. & Hu, J. J. 2011. Walking motion generation, synthesis, and control for biped robot by using PGRL, LPI, and fuzzy logic. *IEEE Transactions on Systems, Man, and Cybernetics, Part B (Cybernetics)* **41**(3), 736–748.

Liu, C., Wang, D. & Chen, Q. 2013. Central pattern generator inspired control for adaptive walking of biped robots. *IEEE Transactions on Systems, Man, and Cybernetics: Systems* **43**(5), 1206–1215.

Michel, O. 2004. WebotsTM: professional mobile robot simulation. *International Journal of Advanced Robotic Systems* **1**(1), 39–42.

Nassour, J., Hugel, V., Ouezdou, F. B. & Cheng, G. 2013. Qualitative adaptive reward learning with success failure maps: applied to humanoid robot walking. *IEEE Transactions on Neural Networks and Learning Systems* **24**(1), 81–93.

Park, K.-H., Jo, J. & Kim, J.-H. 2004. Stabilization of biped robot based on two mode Q-learning. In *Proceedings of the 2nd International Conference on Autonomous Robots and Agents*, 446–451.

Shin, H. K. & Kim, B. K. 2014. Energy-efficient gait planning and control for biped robots utilizing the allowable ZMP region. *IEEE Transactions on Robotics* **30**(4), 986–993.

Su, Y. T., Chong, K. Y. & Li, T. H. S. 2011. Design and implementation of fuzzy policy gradient gait learning method for walking pattern generation of humanoid robots. *International Journal of Fuzzy Systems* **13**(4), 369–382.

Taskiran, E., Yilmaz, M., Koca, O., Seven, U. & Erbatur, K. 2010. Trajectory generation with natural ZMP references for the biped walking robot SURALP. In *Proceedings of 2010 IEEE International Conference on Robotics and Automation (ICRA)*, 4237–4242.

Tedrake, R., Zhang, T. W. & Seung, H. S. 2004. Stochastic policy gradient reinforcement learning on a simple 3D biped. In *Proceedings of 2004 IEEE/RSJ International Conference on Intelligent Robots and Systems*, **3**, 2849–2854.

Vukobratović, M. & Stepanenko, J. 1972. On the stability of anthropomorphic systems. *Mathematical Biosciences* **15**(1), 1–37.